Journal of Stress Analysis
Vol. 6, No. 1, Spring – Summer 2021, 157-166
Bu-Ali Sina University

ORIGINAL RESEARCH PAPER

An Analytical Solution and FEM Simulation for the Behavior of Sensitive FG Micro-valve in Response to pH Stimuli

H. Mazaheri*, K. Soleymani, A. Ghasemkhani
Mechanical Engineering Department, Bu-Ali Sina University, Hamedan, Iran.

Article info

Article history:
Received 07 August 2021
Received in revised form
15 September 2021
Accepted 18 September 2021

Keywords:
pH-sensitive hydrogels
Micro-valve
Functionally graded materials
Analytical solution
Finite element method

Abstract

In this paper, an analytical solution and a numerical simulation of the pH-sensitive hydrogel micro-valves exposed to pH variation are proposed. Case studies consist of micro-valve with homogeneous single-layer and FG hydrogel as the active part. The results of both methods are in good agreement indicating the validity of both methods. In addition, The numerical and analytical solutions were compared between two ranges of cross-linking densities of hydrogels. In order to reach a convergent solution for the finite element model of the micro-valve, the hydrogel layer is considered to have a number of different layers, and an appropriate number of layers are considered. In the next step, parameters affecting the micro-valve behavior are studied, which are the dimensionless thickness ratio, the number of acidic groups in the network, and the salt molarity of the external solution. The findings show that as the thickness ratio, number of acidic groups, and salt concentration in the external solution result increases, the hydrogel part of the micro-valve experiences a higher degree of swelling and deformation, which should be considered when designing these devices.

Nomenclature

$\mathbf{F}$	Deformation gradient tensor	K	Boltzmann constant
$\mathbf{C}$	Right Cauchy-green deformation tensor	$\mathbf{I}_1$	First invariant of $\mathbf{C}$
W_{net}	Free energy density of the network	$J = \det(\mathbf{F})$	Determinant of deformation gradient tensor
W_{sol}	Free energy for mixing between polymer and solvent	$\mathcal{X}$	Interaction parameters with material constants
W_{ion}	Free energy for mixing between ions and solvent	N_{ν_0}, N_{ν_1}	Cross-linking density values in the inner and the outer radii of the shell
W_{dis}	Free energy due to dissociation of the acidic groups of the network	C_q^{ref}	Reference value for true concentration of the specie q
N	Cross-linking density of the hydrogel network	R, r	Radial coordinates in the initial and deformed states.
ν_s	Volume of a water molecule	A, B	Inner and outer radii

*Corresponding author: H. Mazaheri (Assistant Professor)
E-mail address: h.mazaheri@basu.ac.ir
http://dx.doi.org/10.22084/jrstan.2021.25153.1198
ISSN: 2588-2597

C_q	Nominal concentration of the specie q	$\lambda_r, \lambda_\theta$	Radial and Tangential stretches
c_q	True concentration of the specie q	P_r, P_θ	Radial and Tangential stresses
$\boldsymbol{\sigma}$	True stress tensor	$\mathbf{P}$	Fisrt Piola nominal stress tensor

1. Introduction

Hydrogels are a type of elastomers that tend to absorb water and swell in response to chemical and physical stimuli. In some cases, hydrogels can absorb water up to 1000 times greater than their mass and swell without dissolving in water [1]. Due to these properties, they are widely used as sensors and actuators. Swelling in hydrogels is attributed to their hydrophilic nature. The amount of hydrogel swelling is a function of environmental stimuli such as pH [2, 3], temperature changes [4], electric field [5-7], mechanical load [8], light intensity [9], and magnetic field [10]. Therefore, they can comprise the responsive part of various devices such as micro-valves [11-13].

Hydrogels are classified into neutral or ionic ones based on the chemical groups attached to the hydrogel network. Ionic hydrogels respond to pH variation and are divided into three groups, including anionic [14], cationic [15], and ampholytic [16]. As mentioned above, one of the environmental stimuli of hydrogels is pH. Anionic and cationic hydrogels have acidic and basic groups on their polymer networks, respectively. Ampholytic hydrogels, however, are considered to be a combination of anionic and cationic hydrogels. A sudden change in the ionization degree of the hydrogel at a certain pH, denoted by the symbol Pka or Pkb, creates an electrostatic repulsion force between the ions, leading to osmotic force, and then rapid changes occur; this phenomenon leads to a change in the volume of the hydrogel. Anionic hydrogels experience swelling when the pH of the environment exceeds Pka whereas cationic hydrogels swell when the pH of the environment is less than Pkb [17]. It should be noted that the swelling of hydrogel continues up to the point when the elastic forces of the structural network and the cross-linking of the hydrogel prevent further water absorption, impeding the complete dissolution of the hydrogel in water [7].

A proper design of hydrogel devices can be achieved provided that the behavior and fluid flow of hydrogels is accurately modeled. Thus, some main models regarding hydrogel behavior have recently been proposed [18-22].

A general review of hydrogels in [23] provides more information on research and studies in this field. Hong et al. [24] studied the swelling behavior of polyelectrolyte gels and proposed a suitable comprehensive model for these materials in light of their electrochemical basis. In another study [15], researchers developed an efficient model for pH-sensitive cationic hydrogels which was able to simulate swelling behavior of hydrogel in a microchip. In a similar study [25], scientists examined non-uniform swelling behavior for pH-sensitive hydrogels. In some studies predicated upon the results of Beebe et al. [26], the swelling of the hydrogel coating placed on a pillar was investigated. Marcombe et al. [1] presented a theory for pH-sensitive hydrogels and investigated the behavior of the micro-valve introduced by Beebe et al. [26]. Mazaheri et al. [27] investigated the swelling of a temperature-sensitive microvalve through a parametric study. Arbabi et al. [17] also studied a pH-sensitive hydrogel micro-valve and presented some inventive valves with new compositions and arrangements.

The study of FG layered hydrogels has also been a subject of interest [28, 29]; accordingly, smart hydrogel materials with different cross-linking densities can be properly employed in structures under bending. Shojaeifard et al. [30] investigated the bending of sensitive FG hydrogel exposed to environmental stimuli and proposed a semi-analytical method to create pH-sensitive FG micro-beams.

Mazaheri et al. also presented numerical and analytical solutions for a temperature-sensitive FG microvalve [31]. They modeled an incorporated cylindrical FG hydrogel with various cross-linking densities along the radius. Additionally, in another study, Mazaheri et al. [32] researched the swelling of the photothermal sensitive cylindrical polyelectrolyte hydrogel micro-valve and presented an analytical solution for swelling of the hydrogel cylinder exposed to temperature variations and various light intensities. Wu et al. [33] also studied the swelling of an FG hydrogel in which the properties changed along the thickness. Furthermore, Namdar [34] investigated the kinetic of swelling of temperature-sensitive FG cylindrical hydrogels and suggested that the response time can be manipulated by changing the properties of material along the radius of the cylinder.

Due to the unique swelling capability of up to a hundred times their weight when they are immersed in water and are exposed to stimuli, researchers have developed microvalves to control fluid flow in microchannels, in which controlling fluid is laborious. As shown in Fig. 1, the hydrogel is wrapped around support, and the system is placed inside the channel. After introducing the water to the environment and changing the stimuli, the hydrogel starts to absorb water and swells. Finally, it swells to the extent that the gel's outer radius touches the channel wall and seals it. The main advantage of this system is its reversibility in a

way that if the stimuli change to the initial state, the hydrogel swells, and the fluid can thus flow through the channel.

This study aims to present analytical and numerical solutions for swelling of pH-sensitive hydrogel microvalve resulting from the changes in environmental conditions. The micro-valve design used here is the one designed by Beebe et al. [26].

2. pH-Sensitive Hydrogel Modeling

To present the theory of swelling of pH-sensitive hydrogels, it is necessary to introduce the Helmholtz free energy density. Given the model proposed by Marcombe et al. [1], the Helmholtz free energy density is defined as:

$$\begin{aligned} W &= W(F, C_+.C_{H+}, C_-) \\ &= W_{net}(F) + W_{sol}(F) + W_{ion}(F, C_+, C_{H+}, C_-) \\ &+ W_{dis}(F, C_+, C_{H+}, C_-) \end{aligned} \tag{1}$$

where W_{net} is the free energy density caused by the deformation of the hydrogel network, W_{sol} is associated with the mixing of the solvent with the polymer chains of the hydrogel network, W_{ion} is the energy of mixing between the ions and the solvent, and W_{dis} is the energy released by the dissociation of the hydrogel acidic groups. In this function, F represents the deformation gradient tensor, C_+, C_{H+}, and C_- are the nominal concentrations of positive ions, hydrogen ions, and negative ions in the hydrogel, respectively [1]. The density of free energy due to the deformation of the network is expressed as:

$$W_{net} = \frac{1}{2} NKT[I_1 - 3 - 2\log(J)] \tag{2}$$

where NKT is the elastic modulus of pH-sensitive hydrogel, and $\mathbf{I}_1$ is the first invariant of the right-hand Green Cauchy tensor of deformation $C = F^T F$. In this equation, N is the number of polymer chains divided by the volume of the dry network, K is the Boltzmann constant, and T is the absolute temperature. The density of free energy produced as a result of the mixing of solvent molecules with polymer chains is expressed as follows [1]:

$$W_{sol} = \frac{KT}{\nu_s} \left((\det F - 1) \log \left(1 - \frac{1}{\det F} \right) - \frac{\mathcal{X}}{\det F} \right) \tag{3}$$

where ν_s is the volume of a solvent molecule, $\mathcal{X}$ is the dimensionless parameter for mixing polymers and the molecules of the solvents. By considering the concentration of fluid ions, the mixing energy of the ions W_{ion}, is expressed as follows [1]:

$$\begin{aligned} W_{ion} = KT \Bigg[& C_{H+} + \left(\log \frac{C_{H+}}{C_{H+}^{ref} \det F} - 1 \right) \\ & + C_+ \left(\log \frac{C_+}{C_{H+}^{ref} \det F} - 1 \right) \\ & + C_- \left(\log \frac{C_-}{C_-^{ref} \det F} - 1 \right) \Bigg] \end{aligned} \tag{4}$$

where C_{H+}^{ref}, C_+^{ref}, and C_-^{ref} are the reference values of hydrogen ions, positive ions, and negative ions, respectively. The free energy generated by the dissociation of the acidic group is defined as [1]:

$$\begin{aligned} \gamma &= -KTLn \left(\frac{N_a K_a}{C_+^{ref}} \right) \\ W_{dis} &= KT \Bigg[C_{A^-} \log \left(\frac{C_{A^-}}{C_{A^-} + C_{AH}} \right) \\ &+ C_{AH} \log \left(\frac{C_{AH}}{C_{A^-} + C_{AH}} \right) \Bigg] + \gamma C_{A^-} \end{aligned} \tag{5}$$

where C_{AH} and C_{A^-} are the nominal concentrations of acidic groups and constant charges on the hydrogel network and, represents the increase in enthalpy caused by the dissociation of acidic groups. Also K_a is the dissociation constant and has the same as the concentration (mole per liter). It should be noted that, as the hydrogel are considered electrically neutral, the relations $C_{H+} + C_+ = C_{A^-} + C_-$ and $C_{AH} + C_{A^-} = f/\nu$ are established. In the mentioned equations, f denotes the number of acid groups on each chain divided by the total number of monomers in that chain, and $\boldsymbol{\nu}$ is the volume of monomer molecules which is considered to be equal to νs.

The number of α ions (assumed to be present in the hydrogel in the swollen state) divided by the volume of the dry (non-swollen) network determines the nominal concentration of the C_q ions. By dividing C_q by the volume of hydrogel in the swollen state, the true concentration of ion c_q is obtained. The relationship between these two values is defined as: $C_q = c_q \det(\mathbf{F})$. Considering the Avogadro number, NA, the mole concentration of the specie α ion is denoted by $[\alpha]$ and is defined as $C_{H^+} = N_A[H^+]$. By simplifying the above equations, Donnan equations are obtained in the form of Eq. (6) [1]:

$$\begin{aligned} \frac{C_-}{C_-^{ref}} &= \left(\frac{C_{H^+}}{C_{H+}^{ref}} \right)^{-1} \\ \frac{C_+}{C_+^{ref}} &= \left(\frac{C_{H^+}}{C_{H+}^{ref}} \right) \end{aligned} \tag{6}$$

Nominal stress tensor is obtained by differentiating the free energy density with respect to deformation gradient as:

$$\mathbf{P} = \frac{\partial W}{\partial \mathbf{F}} \tag{7}$$

The relationship between real stress $\boldsymbol{\sigma}$ and nominal stress $\mathbf{P}$ is $\boldsymbol{\sigma} = (\det(\mathbf{F}))^{-1}\mathbf{P}\mathbf{F}^T$; the true stress statement is derived from the mentioned relation as [1]:

$$\sigma_{ij} = \frac{NKT}{J}(F_{ik}F_{jk} - \delta_{ij}) + \frac{kT}{\nu_s}\left\{\log\left(1 - \frac{1}{\det \mathbf{F}}\right) + \frac{1}{\det \mathbf{F}} + \frac{\chi}{(\det \mathbf{F})^2}\right\}\delta_{ij} + KT(C_{H^+} + C_+ + C_- - \bar{C}_{H^+} - \bar{C}_+ - \bar{C}_-)\delta_{ij} \tag{8}$$

Substituting Donnan equations in the dissociation equation with the assumption of chemical equilibrium between the gel and the solvent, there is [1]:

$$\frac{C_{H^+}(C_{H^+} + C_+ - C_-)}{(f/\nu)/(\det \mathbf{F})^{-1} - (C_{H^+} + C_+ - C_-)} = N_A K_A \tag{9}$$

which is a cubic equation in terms of C_{H^+}. In numerical and analytical calculations, the volume of each monomer, ν, is considered to be the same as the volume of the solvent molecule, νs. Electro-neutrality of the external solution gives $\bar{c}_- = \bar{c}_{H^+} + \bar{c}_+$. Accordingly, the state of the external solution is determined by two parameters: the concentration of positive ions, $\bar{c}_+$,(or salt concentration) and the concentration of hydrogen ions, $\bar{c}_{H^+}$, (or pH of the external solution). The pH equation of the external solution is presented as $\bar{c}_{H^+} = N_A \times 10^{-pH}$. With the value of external solution pH and salt concentrations in hand and with the help of the constitutive law of the hydrogel, the stress field of the network can be obtained. In the following, material properties of the pH-responsive hydrogel are taken from [1] and presented in Table 1.

3. Analytical Solution

The micro-valve studied in this work is composed of a pH-sensitive hydrogel shell as an active layer. The hydrogel is constrained at the inner radius of the cylindrical shell while it is free at the outer radius as shown in Fig. 1 in which FG and layered hydrogel design (for FEM analysis) are illustrated in the reference state. The hydrogel has an initial stretch λ_0, with respect to its dry state. This value is obtained by setting the stress to zero for each value of $N\nu$. The cross-linking density of the FG hydrogel has a linear variation in the radial direction as below:

$$N\nu = N\nu_0 + \frac{R - A}{B - A}(N\nu_1 - N\nu_0) \tag{10}$$

where A and B denote the internal and external radii of the hydrogel, respectively, and R is the r-coordinate of the material point in the hydrogel. In this work, it is assumed that $N\nu_0 = 0.01$, $N\nu_1 = 0.001$, and $B/A = 2$.

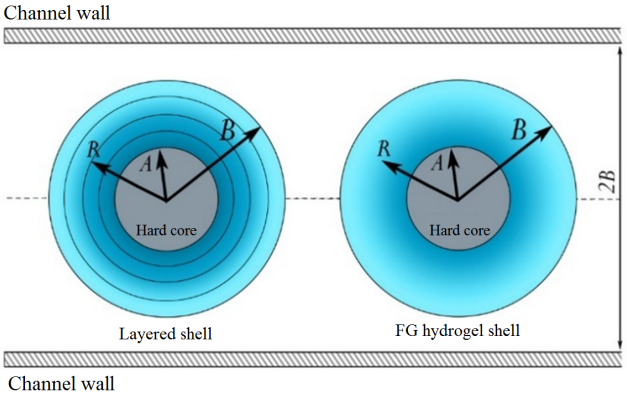

Fig. 1. 2D view from under-study cylindrical hydrogel shells: a) FG hydrogel shell, b) Multi-layer finite element model in the reference state.

The deformation of the hydrogel is assumed to be plane strain due to the confinement in the axial direction of the cylinder. Furthermore, due to the axial symmetry of the micro-valve, the axisymmetric formulation is employed. The reference free-stress state of the micro-valve is considered at pH= 2 for which the free energy function is specified. The equilibrium equation in the radial direction can be written in terms of the nominal radial and hoop stresses of P_r and P_θ:

$$\frac{dP_r}{dR} - \frac{(P_r - P_\theta)}{R} = 0 \tag{11}$$

The mentioned nominal stresses are obtained by differentiating the free energy with respect to the radial and hoop stretches, namely $\lambda_r = \frac{d}{dR}r(R)$, and $\lambda_\theta = \frac{r(R)}{R}$, respectively. Substituting nominal stresses and relevant stretches in the equation of radial equilibrium, a second-order differential equation in terms of $r(R)$ is deduced as:

$$\beta_1 r'' + \beta_2 r^2 \lambda_0^5 (r')^4 + \beta_3 r R \lambda_0^4 (r')^3 - \beta_4 R^2 \lambda_0 (r')^2 + \beta_5 (r') + \beta_6 = 0 \tag{12}$$

Table 1
Material properties of pH-sensitive hydrogel studied in this work [1].

Parameter	$\bar{c}_+$	k_a	f	KT	χ	ν
Value	0.001Molar	4.3	0.03	10^{-21}J	0.1	10^{-28}m^3

where $\Pi = (C_{H^+} + C_+ + C_- - \bar{C}_{H^+} - \bar{C}_+ - \bar{C}_-)$ and $\beta_i s$ are defined as:

$$\begin{aligned}
\beta_1 &= -Nr^2\lambda_0^8 r'^4 + N\nu Rr\lambda_0^5 r'^3 - Nr^2\lambda_0^6 r'^2 \\
&\quad + 2\lambda_0^3 rR(\mathcal{X} + N\nu/2 - 1/2)r' - 2\mathcal{X}R^2 \\
\beta_2 &= (\lambda_0^4 r^2 - R^2\lambda_0^2 + R^2)N\nu + Rr^2\lambda_0^5\Pi' \\
&\quad + R^3\lambda_0 N\nu' + R(2r^2\lambda_0^4\Pi + R^2 N\nu)\lambda_0' \\
\beta_3 &= -(Rr^2\lambda_0^2 N\nu + 2\Pi + 2)\lambda_0' + (Rr^2\lambda_0^3)(N\nu' - \Pi') \\
&\quad + N\nu r^2\lambda_0^3 - Rr^2\lambda_0^2 + R^2(2\mathcal{X} + N\nu - 1) \qquad (13) \\
\beta_4 &= -Rr^2\lambda_0^2(4\mathcal{X} + N\nu - 1)\lambda_0' + 2Rr^2\lambda_0^3 N\nu' \\
&\quad + r^2\lambda_0^3(2\mathcal{X} + N\nu - 1) + \mathcal{X}R^2 \\
\beta_5 &= -Rr^3\lambda_0^8(RN\nu\lambda_0' + R\lambda_0 N\nu' + \lambda_0 N\nu)(r')^4 \\
&\quad - 2\mathcal{X}R^3 r(2R\lambda_0' - \lambda_0) \\
\beta_6 &= +2Rr^3\lambda_0^6\lambda_0'(r')^3(-\lambda_0^3 rr' \\
&\quad + R)\left(\log\left(\frac{\lambda_0^3 rr' - R}{\lambda_0^3 rr' + R}\right)\right)
\end{aligned}$$

In the above equations, $(\,)'$ and $(\,)''$ represent 1st and 2nd differentiation with respect to R. The governing equation will be solved once the boundary conditions are defined. The hydrogel shell is stress-free at the outer radius since the outer radius is unconstrained and can freely swell and deform. Furthermore, due to the rigid attachment of the hydrogel to the hard core, the inner radius remains constant throughout the process. These two boundary conditions along with the obtained 2nd ODE formed a nonlinear boundary value problem that can be solved with appropriate tools. To solve the ODE, finite difference method is employed in MAPLE software for boundary value problem. The obtained analytical results for the considered FG are shown in Fig. 2. The solution for the homogeneous shells with the cross-linking densities equal to the inner and outer radii of the FG cases presented in Fig. 2. As expected, the results for FG and homogeneous shells are different from those for the FG shell. As shown in the figure, the FG solution is within two homogeneous states, which are acceptable for this problem. Note that the stresses are normalized by dividing the true stresses by KT/ν.

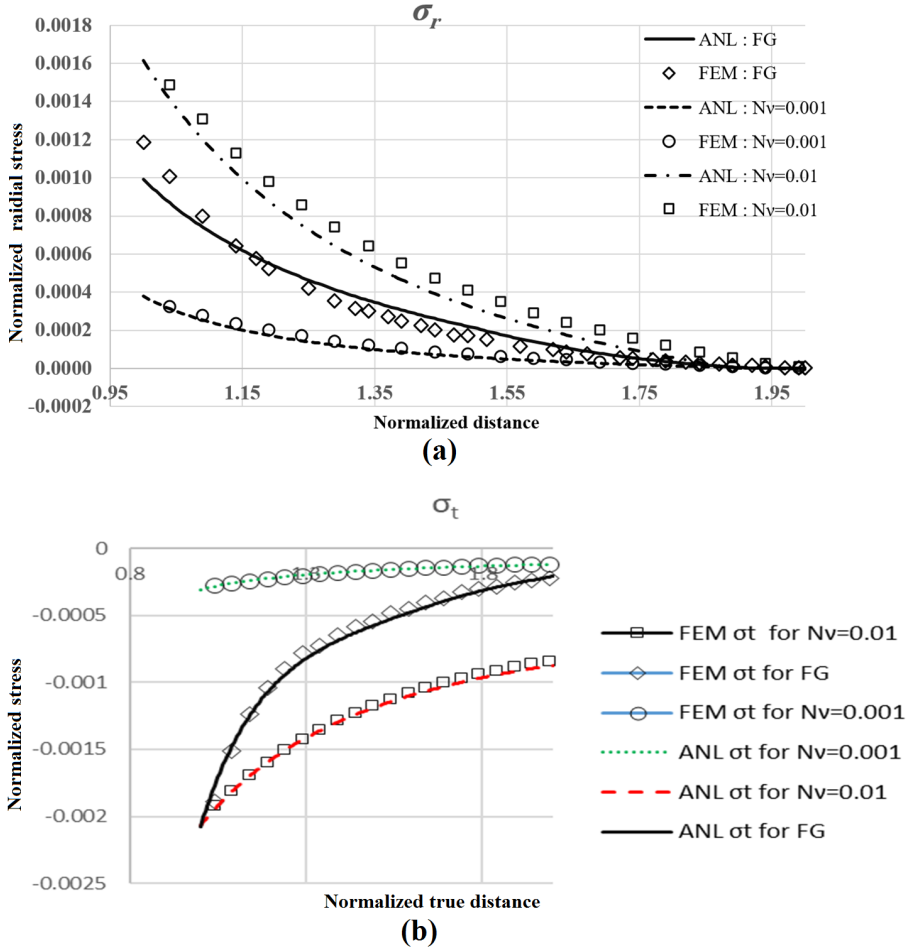

Fig. 2. Comparison between normalized stress based versus the normalized distance: a) Normalized radial stress and, b) Normalized tangential stress for both analytical (ANL) and FEM method for FG and homogeneous cases with $N\nu = 0.01$ and $N\nu = 0.001$ when $B/A = 2$.

4. Numerical Simulation

In this study, numerical solutions were performed using finite element methods via ABAQUS as a commercial FEM software. The obtained results were used to verify the validity of analytical solutions. In this regard, as Fig. 5 illustrates, boundary conditions were defined in finite element simulations for a cylindrical hydrogel shell with a rigid core: the outer radius of the hydrogel shell was considered stress-free in the radial direction.

The behavior of the hydrogel corresponds to a hyperelastic compressible material simulated in ABAQUS software with a UHYPER subroutine. Therefore, the UHYPER subroutine is used to model the behavior of hydrogels in FEM simulations in ABAQUS. To develop the UHYPER, one should provide energy statement (U) and its derivative with respect to the deformation gradient invariants (UI1, UI2, and UI3) in the subroutine. Moreover, note that the energy statement should be rewritten with respect to the initial swollen configuariton network with initial strectch of λ_0. The procedure of manipulating the employed subroutine was depicted in Fig. 3. It should be noted that in the numerical model of the micro-valve, elements of CPE8RH type, which are suitable for the 2D problems of plane strain type were used.

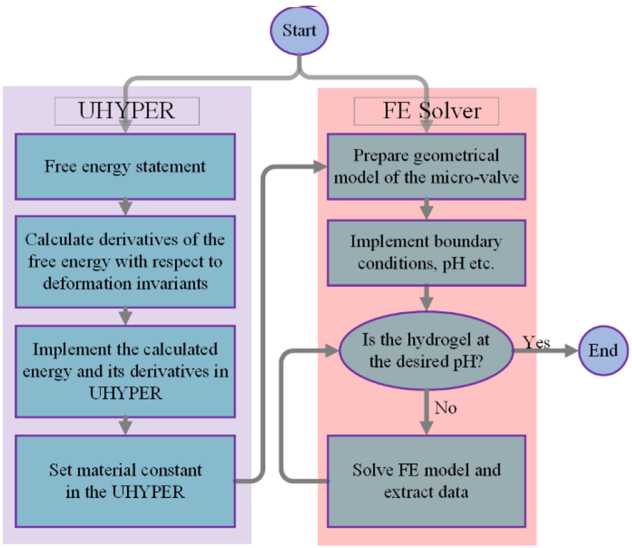

Fig. 3. Flow-chart of numerical simulation procedure.

The obtained results of analytical and numerical methods are presented in Fig. 4 for free swelling problem beside the results of reference [1]. Very good agreement between this work and Marcombe et al. [1] work is observed that guarantees the validity of the obtained results.

As shown in Fig. 1 and Fig. 5, the FG hydrogel is modeled by considering a multi-layer hydrogel shell with different cross-linking densities. In the reference state of pH= 2, each layer has a different initial swelling ratio that should be considered in the UHYPER subroutine. It should be noted that the relative displacement of the different layers of the hydrogel is also considered zero, meaning there is no relative motion between the layers. The inputs of simulation also includes pH variations, ranging from pH = 2 to pH= 8.

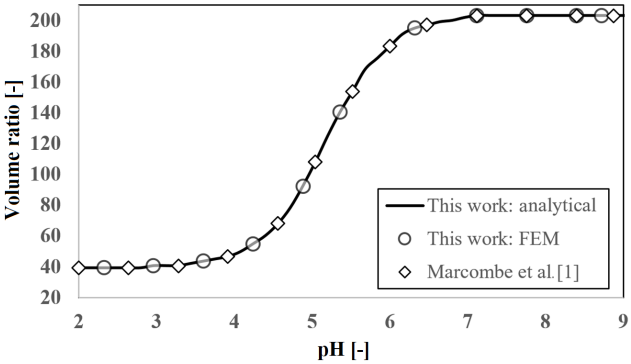

Fig. 4. Comparison between results of this work and Marcombe et al. [1] work.

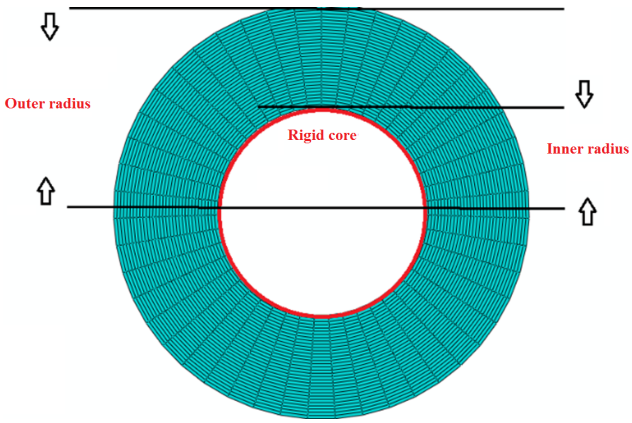

Fig. 5. FEM model of the micro-valve and relevant boundary conditions for a 32-layer hydrogel with a rigid core and a free outer edge in x and y directions.

To obtain the appropriate number of layers at $B/A = 2$, stratifications of 4, 8, 16, to 32 layers were simulated. Based on the simulations, by considering 32 layers for the FG micro-valve, the FEM results are in very good agreement with the analytical method. Thus, for numerical simulation of the FG hydrogel, a 32 layered shell was constructed for FEM simulations.

Fig. 5 also shows boundary conditions for the 32-layered shell with $B/A = 2$: the outer radius was considered stress free and the inner radius of the shell has zero displacements. The numerical results for FG micro-valve and two homogeneous limit cases with $N\nu = 0.001$ and $N\nu = 0.01$ are obtained and depicted in Fig. 2. As shown in Fig. 2, there is excellent agreement between the numerical and analytical solutions, verifying the validity of both methods. Thereby, the procedures applied in both numerical and analytical solutions are proved acceptable and reliable.

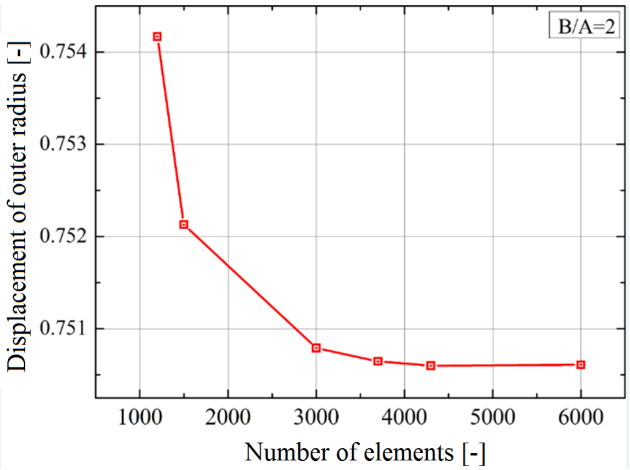

Fig. 6. Mesh independence study for a 32-layered FG hydrogel with a radius ratio of $B/A = 2$.

It is worth noting that, in the finite element simulation, the obtained results must be independent of the mesh size. Therefore, the mesh size was also selected in a way that does not affect the final results. Fig. 6 indicates the mesh size effect on the displacement of the outer radius of the micro-valve. According to this diagram, the results are almost independent of the mesh dimensions when the number of elements is 6000. Therefore, for the next subsequent simulations, the number of elements is considered to be at least 4500 so that the results are sufficiently accurate.

5. Results and Discussion

In this section, the results of the study are discussed, and some parametric studies will be presented for the FG and homogeneous micro-valves. Both analytical and numerical methods are considered for the homogeneous shell with $N\nu = 0.01$ and $N\nu = 0.001$ as well as FG hydrogel.

There is a good agreement between numerical and analytical methods as shown in Fig. 2, verifying the validity of both methods.

As can be seen in Fig. 2, the tangentially normalized stress σ_t increases from the beginning of the inner radius of the rigid core of the hydrogel through the outer radius of the hydrogel. On the other hand, σ_r decreases as the radius increases toward the outer layers of the hydrogel and approaches zero on the outer radius of the micro-valve. As to other results, it can be deduced that the results of finite element solution and analytical solution have a very good agreement for all homogeneous and FG micro-valves. On the other hand, the analytical solution of FG hydrogel lies between two analytical solutions with cross-linking densities of $N\nu = 0.01$ and $N\nu = 0.001$. Obviously, on the radius close to the outer edge of the hydrogel, all the curves of radial stress approach zero, which results from zero stress boundary conditions at the outer edge of the hydrogel.

5.1. Investigation of the Effect of Thickness Ratio

Now, the effect of some parameters on the swelling behavior of the hydrogel micro-valve can be studied. To do so, one of the important geometric characteristics of the micro-valve, hydrogel external radius- internal radius ratio will be considered, which is represented by B/A. This parameter has a vital role in the determination of the closing pH of a specified micro-valve with a given width of the micro-valve. Different outer radius- inner radius ratios were considered for dimensionless values of $B/A = 1.2$, $B/A = 1.5$, $B/A = 2.0$, and $B/A = 2.5$. The results are shown in Figs. 7-10 for normalized outer radius of the hydrogel which is defined as ratio of the current outer radius of the hydrogel to A. Similar to the previous section, the results are presented for the FG hydrogel as well as two homogeneous cases with $N\nu = 0.01$ and $N\nu = 0.001$. The curves have a similar trend, but for the thicker hydrogels, the FG hydrogel behavior approaches the behavior of homogeneous cases $N\nu = 0.001$. On the other hand, for a lower value of thickness ratio, the FG behavior is more similar to the homogeneous case with $N\nu = 0.01$; this is due to more confinement of the shell with a lower thickness ratio that is sensed by the hydrogel, resulting in a lower amount of swelling.

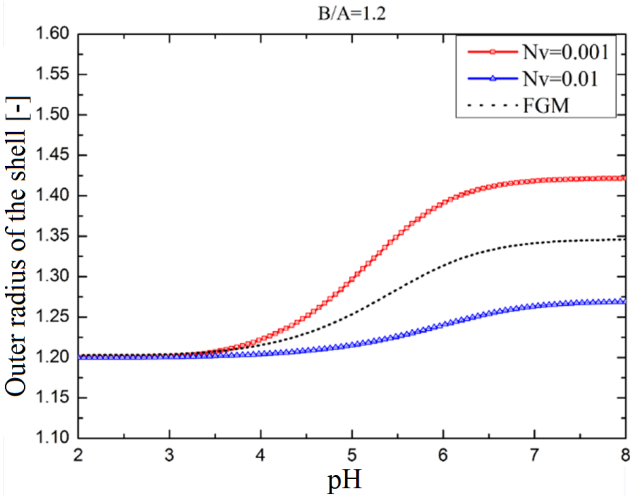

Fig. 7. Normalized outer radius of the hydrogel shell in FG and homogeneous solutions for radius ratio of $B/A = 1.2$ versus to pH changes.

In addition, by examining Figs. 7-10, it can be concluded that the higher the thickness ratio of the hydrogel is, the more external radius displacement of the hydrogel will be for certain pH changes. Furthermore, the displacement of the outer layer of the hydrogel is larger for the homogeneous case with the lower cross-linking density as expected due to the high capacity of this hydrogel for swelling. On the other hand, all

curves show a transition within the pH range of 3-6, which is in agreement with the transition characteristic of this material. These conclusions are valuable in the applications mentioned in the introduction section, especially in medicine, pharmacotherapy, and micro-valve.

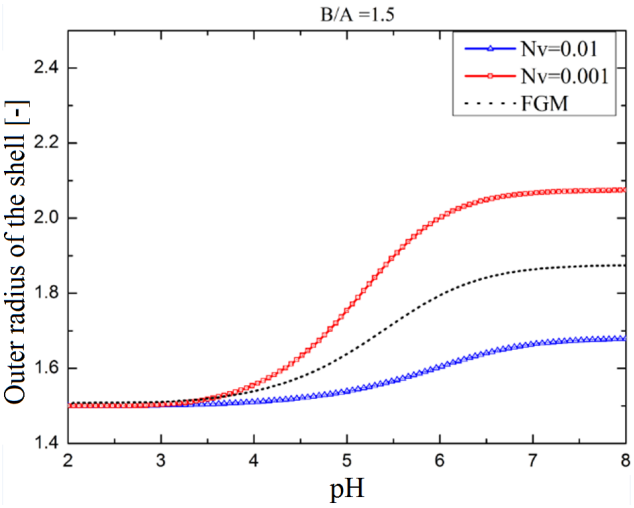

Fig. 8. Normalized outer radius of the hydrogel shell in FG and homogeneous solutions for radius ratio of $B/A = 1.5$ versus to pH changes.

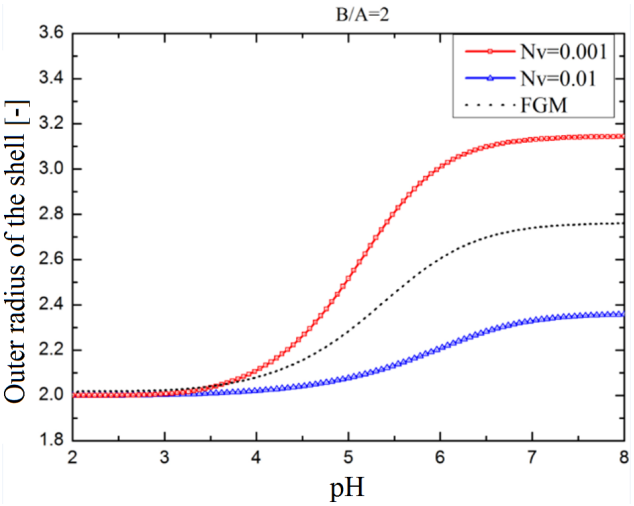

Fig. 9. Normalized outer radius of the hydrogel shell in FG and homogeneous solutions for radius ratio of $B/A = 2$ versus to pH changes.

5.2. Investigation of the Effect of Acidic Group Number

In the previous section, the amount of swelling the hydrogel experiences was examined for different values of B/A and different cross-linking densities. Still, another parameter to consider in the study of FG micro-valve is the amount of acid group attached to the hydrogel network represented by f as mentioned in the hydrogel constitutive modeling formulation. As shown in Fig. 11, as the amount of f rises, the swelling and displacement of the outer radius of the micro-valve increase. This is due to the increased level of hydrogel sensitivity to pH variations. As the number of acidic groups goes up, a more fixed charge on the network will be generated, caused by acidic dissociation. As a result, more repulsion forces are generated on the network, leading to more solvent absorption on the network and more swelling.

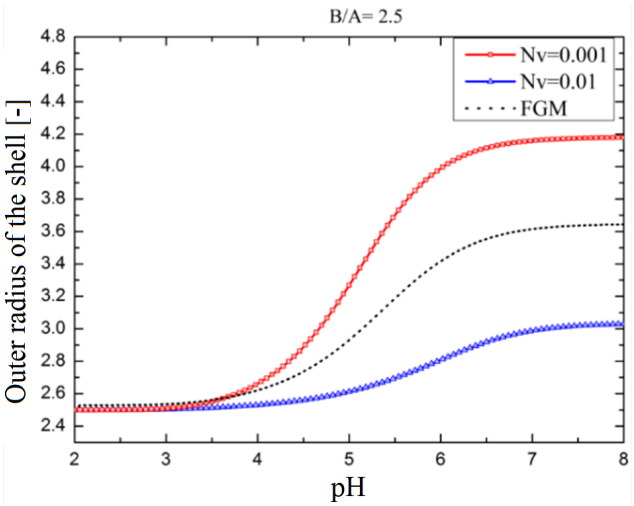

Fig. 10. Normalized outer radius of the hydrogel shell in FG and homogeneous for radius ratio of $B/A = 2.5$ versus to pH changes.

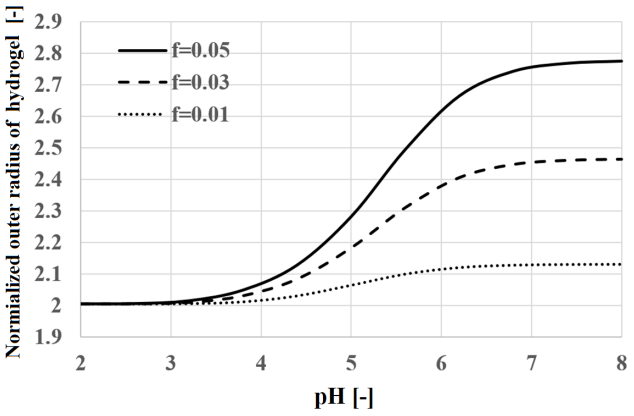

Fig. 11. Investigation of the effect acidic group of the network in the swelling behavior of the FG hydrogel cylinder.

5.3. Investigation of Salt Molarity of the External Solution

Besides the acidic group number, the salt concentration of the external solution can affect the behavior of the micro-valve. Thus, this section investigates how the salt molarity of the external solution affects the results. Fig. 12 illustrates the findings. As the results show, increasing the salt molarity causes less swelling of the micro-valve in higher values of pH. This decrease stems from the Donnan effect and electro-neutrality of

the external solution and the hydrogel. For lower values of pH, salt molarity of the external solution has no considerable effect due to existence of proton ion in the environment. On the other hand, for basic environment (higher pH value), acidic groups start to dissociate and swelling of the network occurs. Yet, electroneutrality of the network and the solution beside Donnan conditions results in lower swelling of the network for larger salt contents of the external solution. Thus, all the discussed parameters need to be considered to achieve a more accurate design of the FG micro-valve.

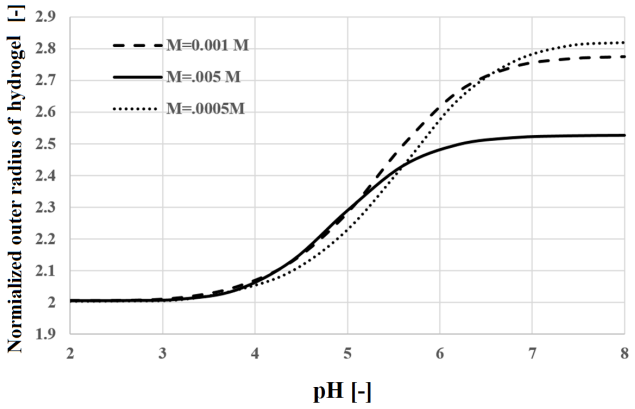

Fig. 12. Investigation of the effect of salt concentration on the swelling behavior of the FG hydrogel cylinder.

6. Conclusions

Hydrogels are a type of gels which swell by absorbing the surrounding fluids. The general behavior of these materials in the swollen state is similar to that of soft elastic solids.

In this work, the pH-sensitive micro-valve was studied: the active hydrogel part of the valve responds to pH variations as the volume changes, leading to the opening or closing of the micro-valve. In this regard, the theoretical relationships governing the behavior of hydrogel micro-valves were presented, and an analytical solution was proposed for the swelling behavior of the under-study micro-valve. Besides, numerical simulation of the pH-sensitive micro-valve was performed for pH values ranging from 2 to 8 with UHYPER in ABAQUS. A very good agreement between the two methods was observed, guaranteeing the validity of both methods. Then, an appropriate number of layers were selected for the FG micro-valve by conducting a parametric study on the number of layers in the FEM model of FG hydrogel. Then, for the FG micro-valve, a parametric study was carried out to evaluate the effects of thickness ratio of the active hydrogel layer, the number of acidic groups of the hydrogel network, and the external solution molarity. The obtained results were discussed and explained on the basis of physical phenomena that exist in hydrogel swelling, especially for the under-study pH-sensitive ones. As discussed in the previous section, for thicker hydrogels, more swelling was observed due to less confinement of the hydrogel. As number of the acidic groups increased, the swelling of the micro-valve also increased. On the other hand, the external solution salt content affected the swelling of the micro-valve in a complicated manner that was dependent on the pH value of the environment.

References

[1] R. Marcombe, S. Cai, W. Hong, X. Zhao, Y. Lapusta, Z. Suo, A theory of constrained swelling of a pH-sensitive hydrogel, Soft Matter, 6(4) (2010) 784-793.

[2] W. Otto, L. Drahoslav, Cross-linked hydrophilic polymers and articles made therefrom, (1965), Google Patents.

[3] H. Mazaheri, A. Ghasemkhani, S. Sabbaghi, Study of fluid–structure interaction in a functionally graded pH-sensitive hydrogel micro-valve, Int. J. Appl. Mech., 12(05) (2020) 2050057.

[4] T. Morimoto, F. Ashida, Temperature-responsive bending of a bilayer gel, Int. J. Solids Struct., 56 (2015) 20-28.

[5] F. Lai, H. Li, R. Luo, Chemo-electro-mechanical modeling of ionic-strength-sensitive hydrogel: Influence of Young's modulus, Int. J. Solids Struct., 47(22-23) (2010) 3141-3149.

[6] X. Zhou, Y.C. Hon, S. Sun, A.F.T. Mak, Numerical simulation of the steady-state deformation of a smart hydrogel under an external electric field, Smart Mater. Struct., 11(3) (2002) 459-467.

[7] A. Kargar-Estahbanaty, M. Baghani, H. Shahsavari, Gh. Faraji, A combined analytical-numerical investigation on photosensitive hydrogel microvalves, Int. J. Appl. Mech., 9(07) (2017) 1750103.

[8] M. Doi, Gel dynamics, J. Phys. Soc. Jpn., 78(5) (2009) 052001.

[9] H. Mazaheri, A.H. Namdar, A. Ghasemkhani, A model for inhomogeneous large deformation of photo-thermal sensitive hydrogels, Acta Mech., 232 (2021) 2955-2972.

[10] T.Y. Liu, S.H. Hu, T.Y. Liu, D.M. Liu, S.Y. Chen, Magnetic-sensitive behavior of intelligent ferrogels for controlled release of drug. Langmuir, 22(14) (2006) 5974-5978.

[11] P. Gupta, K. Vermani, S. Garg, Hydrogels: from controlled release to pH-responsive drug delivery, Drug Discov. Today, 7(10) (2002) 569-579.

[12] H. Mazaheri, A. Khodabandehloo, FSI and non-FSI studies on a functionally graded temperature-responsive hydrogel bilayer in a micro-channel, Smart Mater. Struct., 31(1) (2022) 015007.

[13] H. Mazaheri, A.H. Namdar, A. Amiri, Behavior of a smart one-way micro-valve considering fluid–structure interaction, J. Intell. Mater. Syst. Struct., 29(20) (2018) 3960-3971.

[14] S.K. De, N.R. Aluru, B. Johnson, W.C. Crone, D.J. Beebe, J. Moore, Equilibrium swelling and kinetics of pH-responsive hydrogels: Models, experiments, and simulations, J. Microelectromechanical Syst., 11(5) (2002) 544-555.

[15] A. Drozdov, Swelling of pH-responsive cationic gels: Constitutive modeling and structure–property relations, Int. J. Solids Struct., 64 (2015) 176-190.

[16] H. Yan, B. Jin, S. Gao, L. Chen, Equilibrium swelling and electrochemistry of polyampholytic pH-sensitive hydrogel, Int. J. Solids Struct., 51(23-24) (2014) 4149-4156.

[17] N. Arbabi, M. Baghani, J. Abdolahi, H. Mazaheri, M. Mosavi-Mashhadi, Study on pH-sensitive hydrogel micro-valves: A fluid-structure interaction approach, J. Intell. Mater. Syst. Struct, 28(12) (2017) 1589-1602.

[18] S. Cai, Z. Suo, Mechanics and chemical thermodynamics of phase transition in temperature-sensitive hydrogels, J. Mech. Phys. Solids, 59(11) (2011) 2259-2278.

[19] S.A. Chester, L. Anand, A thermo-mechanically coupled theory for fluid permeation in elastomeric materials: application to thermally responsive gels, J. Mech. Phys. Solids, 59(10) (2011) 1978-2006.

[20] H. Mazaheri, M. Baghani, R. Naghdabadi, S. Sohrabpour, Inhomogeneous swelling behavior of temperature sensitive PNIPAM hydrogels in micro-valves: Analytical and numerical study, Smart Mater. Struct., 24(4) (2015) 045004.

[21] R. Xiao, J. Qian, S. Qu, Modeling gel swelling in binary solvents: a thermodynamic approach to explaining cosolvency and cononsolvency effects, Int. J. Appl. Mech., 11(5) (2019) 1950050.

[22] S. Zheng, Z. Li, Z. Liu, The fast homogeneous diffusion of hydrogel under different stimuli, Int. J. Mech. Sci., 137 (2018) 263-270.

[23] Z. Liu, W. Toh, T.Y. Ng, Advances in mechanics of soft materials: A review of large deformation behavior of hydrogels, Int. J. Appl. Mech., 7(05) (2015) 1530001.

[24] W. Hong, X. Zhao, Z. Suo, Large deformation and electrochemistry of polyelectrolyte gels. J. Mech. Phys. Solids, 58(4) (2010) 558-577.

[25] A. Drozdov, J.D. Christiansen, The effects of pH and Ionic strength of swelling of cationic gels, Int. J. Appl. Mech., 8(5) (2016) 1650059.

[26] D.J. Beebe, J.S. Moore, J.M. Bauer, Q. Yu, R.H. Liu, C. Devadoss, B.H. Jo, Functional hydrogel structures for autonomous flow control inside microfluidic channels, Nature, 404(6778) (2000) 588-590.

[27] H. Mazaheri, M. Baghani, R. Naghdabadi, S. Sohrabpour, Coupling behavior of the pH/temperature sensitive hydrogels for the inhomogeneous and homogeneous swelling, Smart Mater. Struct., 25(8) (2016) 085034.

[28] M. Guvendiren, J.A. Burdick, S. Yang, Kinetic study of swelling-induced surface pattern formation and ordering in hydrogel films with depth-wise cross-linking gradient, Soft Matter, 6(9) (2010) 2044-2049.

[29] M. Guvendiren, S. Yang, J.A. Burdick, Swelling-induced surface patterns in hydrogels with gradient cross-linking density, Adv. Funct. Mater., 19(19) (2009) 3038-3045.

[30] M. Shojaeifard, F. Rouhani, M. Baghani, A combined analytical–numerical analysis on multi-directional finite bending of functionally graded temperature-sensitive hydrogels, J. Intell. Mater. Syst. Struct., 30(13) (2019) 1882-1895.

[31] H. Mazaheri, A. Ghasemkhani, Analytical and numerical study of the swelling behavior in functionally graded temperature-sensitive hydrogel shell, J. Stress Anal., 3(2) (2019) 29-35.

[32] H. Mazaheri, A. Ghasemkhani, A.H. Namdar, Behavior of photo-thermal sensitive polyelectrolyte hydrogel micro-valve: Analytical and numerical approaches, J. Stress Anal., 5(1) (2020) 21-30.

[33] Z. Wu, N. Bouklas, R. Huang, Swell-induced surface instability of hydrogel layers with material properties varying in thickness direction, Int. J. Solids Struct., 50(3-4) (2013) 578-587.

[34] A.H. Namdar, Kinetics of swelling of cylindrical functionally graded temperature-responsive hydrogels, J. Comput. Appl. Mech., 51(2) (2020) 464-471.